Sodium Antimony Gluconate Induces Generation of Reactive Oxygen Species and Nitric Oxide via Phosphoinositide 3-Kinase and Mitogen-Activated Protein Kinase Activation in *Leishmania donovani*-Infected Macrophages

Jayati Mookerjee Basu,[1] Ananda Mookerjee,[3] Prosenjit Sen,[2] Suniti Bhaumik,[1] Pradip Sen,[5]
Subha Banerjee,[1] Ksudiram Naskar,[1] Soumitra K. Choudhuri,[3] Bhaskar Saha,[4]
Sanghamitra Raha,[2] and Syamal Roy[1]*

*Department of Immunology, Indian Institute of Chemical Biology, 4 Raja S. C. Mullick Road, Kolkata 700032, India[1]; Department of
Crystallography and Molecular Biology, Saha Institute of Nuclear Physics, Kolkata 700064, India[2]; Department of
Environmental Carcinogenesis and Toxicology, Chittaranjan National Cancer Institute, Kolkata 700026, India[3];
National Centre for Cell Science, Pune 411007, India[4]; and Department of Cell Biology
and Immunology, Institute of Microbial Technology, Chandigarh 160036, India[5]*

Pentavalent antimony complexes, such as sodium stibogluconate and sodium antimony gluconate (SAG), are still the first choice for chemotherapy against various forms of leishmaniasis, including visceral leishmaniasis, or kala-azar. Although the requirement of a somewhat functional immune system for the antileishmanial action of antimony was reported previously, the cellular and molecular mechanism of action of SAG was not clear. Herein, we show that SAG induces extracellular signal-regulated kinase 1 (ERK-1) and ERK-2 phosphorylation through phosphoinositide 3-kinase (PI3K), protein kinase C, and Ras activation and p38 mitogen-activated protein kinase (MAPK) phosphorylation through PI3K and Akt activation. ERK-1 and ERK-2 activation results in an increase in the production of reactive oxygen species (ROS) 3 to 6 h after SAG treatment, while p38 MAPK activation and subsequent tumor necrosis factor alpha release result in the production of nitric oxide (NO) 24 h after SAG treatment. Thus, this study has provided the first evidence that SAG treatment induces activation of some important components of the intracellular signaling pathway, which results in an early wave of ROS-dependent parasite killing and a stronger late wave of NO-dependent parasite killing. This opens up the possibility of this metalloid chelate being used in the treatment of various diseases either alone or in combination with other drugs and vaccines.

Visceral leishmaniasis, caused by *Leishmania donovani*, is fatal if left untreated. The pentavalent antimony (Sb^V) compound urea stibamine first emerged as an effective chemotherapeutic agent against Indian kala-azar (6). Although different forms of pentavalent antimony complexes (chelates, i.e., Sb^V chelated to an organic backbone), namely, sodium stibogluconate (Pentostam) and meglumine antimoniate (Glucantime), are still the first choice for treatment of leishmaniases (21, 42), their mechanism of action is still largely unknown. Previous studies indicated that sodium antimony gluconate (SAG) failed to act in immunocompromised hosts, such as patients who are suffering from AIDS or receiving immunosuppressive agents (17, 38) and nude (36) and severe combined immunodeficient (SCID) mice (15). Several studies have shown that endogenous interleukin-2 (IL-2) (34), IL-4 (1, 43), and IL-12 (41) influence the effectiveness of chemotherapy with pentavalent antimony. These findings are inclined to indicate the requirement of a somewhat functional T-cell compartment for SAG action. Moreover, SAG has been found to inhibit selective protein tyrosine phosphatases (Src homology 2 domain-containing tyrosine phosphatase 1 [SHP1] and SHP2) in vitro and augment cytokine signaling and responses in

hematopoietic cell lines (46), suggesting the role of phosphatases and possibly other signal transduction pathways in SAG-induced control of *Leishmania* infection. In addition, the dose of SAG that kills the axenic amastigotes in vitro is 50 times higher than the concentration of the drug required for killing the parasite within macrophages (Mϕs) (23), suggesting host cell activation as an integral component of SAG-induced antileishmanial effects. Moreover, SAG synergizes with alpha interferon (IFN-α) to activate STAT1 to kill IFN-α-resistant human cancer cell lines, like WM9 (melanoma), SW620 (colon carcinoma), U266 (multiple myeloma), MDA231 (prostate cancer), etc., in vitro (56). These studies indicate that this metalloid chelate might modulate a number of signaling events. Therefore, we assessed whether SAG modulates the signal transduction pathways in macrophages to kill the intracellular parasites. Herein, we report for the first time that SAG triggers activation of phosphoinositide 3-kinase (PI3K), protein kinase C (PKC), and mitogen-activated protein kinases (MAPKs) coupled with the activation of the microbicidal mechanism of Mϕ, which ultimately leads to the elimination of the intracellular *L. donovani* parasites.

MATERIALS AND METHODS

Antibodies and other reagents. Anti-β-actin monoclonal antibody (MAb) was purchased from Sigma (St. Louis, MO). Anti-tumor necrosis factor alpha (TNF-α) MAb and an Opt enzyme immunoassay kit for assay of TNF-α were obtained from BD Biosciences (San Diego, CA). Anti-PI3K and anti-phospho-PI3K (p85) were obtained from Santa Cruz Biotech, Inc. All other antibodies

---

* Corresponding author. Mailing address: Department of Immunology, Indian Institute of Chemical Biology, 4 Raja S. C. Mullick Road, Kolkata 700032, India. Phone: 091-033-2473-3491. Fax: 091-033-2473-5197. E-mail: sroy@iicb.res.in.

(Abs) (anti-Akt, anti-phospho-Akt [Ser473], anti-PKC α, anti-phospho-PKC α/β$_{II}$ [Thr638/641], anti-Raf, anti-phospho-Raf [Ser338], anti-p38 MAPK, anti-phospho-p38 MAPK [Thr180/Tyr182], anti-p42/44 MAPK, and anti-phospho-extracellular signal-regulated kinase [ERK] [Thr202/Tyr204]), inhibitors (U0126 and SB203580), and LumiGlo reagents for chemiluminescence were obtained from Cell Signaling (Beverly, MA). Fetal bovine serum (FBS) was obtained from Invitrogen Corporation (Carlsbad, CA). Inhibitors (wortmannin, calphostin C, and mevastatin), Giemsa stain, Bradford reagent, N-acetylcysteine (NAC), N^G-monomethyl-L-arginine acetate (L-NMMA), EDTA, EGTA, Tris base, N(1-naphthyl)ethylenediaminedihydrochloride, sulfanilamide, sodium orthovanadate (Na$_3$VO$_4$), Triton X-100, phenylmethylsulfonyl fluoride, leupeptin, aprotinin, antipain, N-p-tosyl-phenylalanine chloromethyl ketone (TPCK), Nα-p-tosyl-L-lysine chloromethyl ketone (TLCK), starch, penicillin, streptomycin, medium 199 (M199), RPMI 1640, and trypan blue were obtained from Sigma (St. Louis, MO). 2′,7′-Dichloro dihydrofluorescein diacetate (DCFDA) was obtained from Molecular Probes (Eugene, OR). Preservative-free sodium stibogluconate was the kind gift of Albert David India, Ltd. (Calcutta, India).

Parasites, animals, and cell culture. *Leishmania donovani* MHOM/IN/1983/AG83 (50) parasites were used during the course of this investigation. Amastigotes obtained from spleens of infected hamsters were cultured in M199 containing 20% (vol/vol) heat-inactivated FBS supplemented with 100 IU/ml of penicillin and 100 μg/ml of streptomycin at 22°C to obtain promastigotes (11). Promastigotes were grown in fresh M199 containing 10% (vol/vol) heat-inactivated FBS for 3 to 5 days at 22°C before further experimentation.

BALB/c and C57BL/6 (wild-type and inducible nitric oxide synthase-deficient [iNOS$^{-/-}$]) mice, originally obtained from Jackson Laboratories, Bar Harbor, ME, and reared in the institute animal facilities, were used for experimental purposes with prior approval of the animal ethics committee.

Mφs were isolated from mice 36 to 48 h after injection (intraperitoneal) with 2% (wt/vol) hydrolyzed starch by peritoneal lavage with ice-cold phosphate-buffered saline. Cells were washed and cultured for 18 to 24 h (for adherence) in RPMI 1640 (supplemented with 100 IU/ml of penicillin and 100 μg/ml of streptomycin) containing 10% (vol/vol) heat-inactivated FBS (RPMI-FBS) at 37°C at 5% CO$_2$ in air in tissue culture petri dishes of 65 mm in diameter (Tarson India Ltd.), following which culture medium was washed off and fresh RPMI-FBS was added. About 1 × 10^6 Mφs were cultured in 1 ml of RPMI-FBS. In some experiments, 5 × 10^5 Mφs were maintained on 22-mm by 22-mm cover glass placed in plastic petri dishes.

Infection of Mφs and determination of intracellular parasite numbers. During the course of this study, Mφs were infected with promastigotes at a Mφ-to-parasite ratio of 1:10 in RPMI-FBS, as described elsewhere (11). After 4 h of incubation at 37°C at 5% CO$_2$ in air, unbound parasites were washed off with RPMI and Mφs were then maintained in RPMI-FBS for 22 h at 37°C at 5% CO$_2$ in air. Intracellular parasite numbers were enumerated in Giemsa-stained preparations of samples, as described elsewhere (11, 51).

Treatments. At 22 h postinfection, the Mφs were treated with SAG at a concentration of 10 μg/ml, because this is the highest attainable serum concentration of the drug during chemotherapy of kala-azar patients (4, 46) and we have also previously demonstrated the drug to be cytotoxic in vitro above 10 μg/ml (13). In some experiments, cells were treated with the PI3K inhibitor wortmannin (1 μM) (22), the PKC inhibitor calphostin C (50 nM) (24), the Ras inhibitor mevastatin (5 μM) (20), the p38 MAPK inhibitor SB203580 (5 μM) (47), the MEK-1/MEK-2 inhibitor U0126 (1 μM) (16), L-NMMA (0.4 mM) (18), or anti-TNF-α Ab (10 μg/ml) for 1 h prior to SAG treatment (10 μg/ml) or were treated with NAC (5 mM) (49) along with SAG. The doses of inhibitors mentioned above were found to be nontoxic and were used by others previously (16, 18, 20, 22, 24, 47, 49). We also observed that wortmannin, calphostin C, mevastatin, SB203580, U0126, L-NMMA, and TNF-α Ab were not cytotoxic to Mφs, as evidenced by an MTT (3-[4,5-dimethylthiazol-2-yl]-2,5-diphenyltetrazolium bromide) assay and unaltered Mφ morphology at the above-mentioned doses (data not shown). NAC at the above-mentioned reported dose was found to be nontoxic even after 18 h, as determined by trypan blue exclusion staining.

Measurement of ROS. To monitor the level of reactive oxygen species (ROS) (including superoxide, hydrogen peroxide, and other reactive oxygen intermediates) produced within the cells, the cell-permeable, nonpolar, H$_2$O$_2$-sensitive probe DCFDA was used (53). Extent of H$_2$O$_2$ generation was defined as ROS generation for our convenience. Uninfected Mφs and infected Mφs (I-Mφs), untreated or treated with SAG for various durations, were pretreated in some experiments with wortmannin, calphostin C, mevastatin, U0126, or SB203580 for 1 h or treated with NAC along with SAG. The cells were harvested in Hanks balanced salt solution (HBSS). Finally, 1 × 10^6 cells were placed in 1 ml of HBSS, pulsed with DCFDA (5 μM) for 20 to 30 min at 37°C in the dark, and then washed twice with HBSS; the relative fluorescence was measured by fluo-

rimetry with a fluorimeter (Hitachi) (excitation at 505 nm and emission at 525 nm at a slit size of 1 nm). For each experimental sample, fluorimetric measurements were performed in triplicate and expressed as fluorescent intensity units/10^6 cells.

Measurement of NO. Nitric oxide (NO) generation in response to SAG treatment of Mφs or I-Mφs was monitored by Griess reaction as described previously (18, 19). In some experiments, the cells were treated with wortmannin, calphostin C, mevastatin, U0126, SB203580, anti-TNF-α, or L-NMMA for 1 h prior to SAG treatment. The amount of nitrite accumulated was calculated from a standard curve constructed with different concentrations of sodium nitrite, and the concentration of nitrite accumulated was expressed as μM nitrite.

Preparation of cell lysates and Western blot analysis. Uninfected Mφs or I-Mφs, either untreated or treated with SAG for different durations, were harvested, resuspended in TEEM buffer (32), and rapidly freeze-thawed thrice and passed through a 26-gauge needle (10 times) for lysis. The lysates were centrifuged (800 × g for 10 min at 4°C), the supernatants were collected, and the proteins were estimated using Bradford reagent. The supernatants were mixed with Laemmli buffer, heated in a boiling water bath for 5 min, and cooled to room temperature. About 20 μg of protein was loaded in each lane of sodium dodecyl sulfate-polyacrylamide gels, electrophoresed, and then transferred onto polyvinylidene difluoride membrane. Immunoblotting was performed with appropriately diluted specific primary Abs, and finally chemiluminescence was performed with LumiGlo reagent as described by the manufacturer. Densitometric analyses were done using Quantity1 (Bio-Rad) software.

Assay of cytokines. Uninfected or MHOM/IN/1983/AG83-infected Mφs (1 × 10^6) were treated with SAG for different durations in a final culture volume of 200 μl. The supernatants were collected after centrifugation. Then, TNF-α was assayed using an enzyme-linked immunosorbent assay kit according to the manufacturer's protocol.

Statistical analysis. Each experiment was performed three to five times and results are expressed as means ± standard errors of the means (SEM), or Student's t test for significance was performed and a P value of <0.05 was considered significant. Western blots show representative data from three independent experiments.

RESULTS

SAG-induced generation of ROS and NO in macrophage and control of intracellular parasites. Since ROS and NO are the two major microbicidal molecules (2), we examined whether the antileishmanial effects of SAG were dependent on these two free radicals. It was observed that the amastigotes grew until 24 h after infection in the SAG-untreated I-Mφs, whereas in SAG-treated I-Mφs the amastigote count steadily declined (Fig. 1A), suggesting an early control of the parasite load by SAG.

Since pentavalent antimonial treatment in vitro induces ROS generation in human polymorphonuclear cells (48), we studied the ability of SAG to induce ROS in uninfected Mφs and I-Mφs. We observed that ROS generation was enhanced significantly ($P < 0.001$) in uninfected Mφs upon SAG treatment. The peak was attained at 3 h, and the level decreased gradually thereafter (Fig. 1B). Similarly, there was a slight enhancement of NO generation with time in uninfected Mφs but this was significantly ($P < 0.001$) enhanced upon SAG treatment (Fig. 1C). When I-Mφs were treated with SAG, there was early ROS and late NO generation, which was essentially comparable to observations with SAG-treated uninfected Mφs (Fig. 1B and C). However, there was a slight right shift of the peak of ROS generation, the cause of which is not known (Fig. 1B). Interestingly, as with starch-elicited Mφs, SAG could induce both ROS and NO generation in resident peritoneal Mφs and could induce high levels of ROS generation in P388D1 cells (data not shown).

To ascertain that ROS is indeed involved in the early-hour killing of *L. donovani*, I-Mφs were treated with NAC, a potent
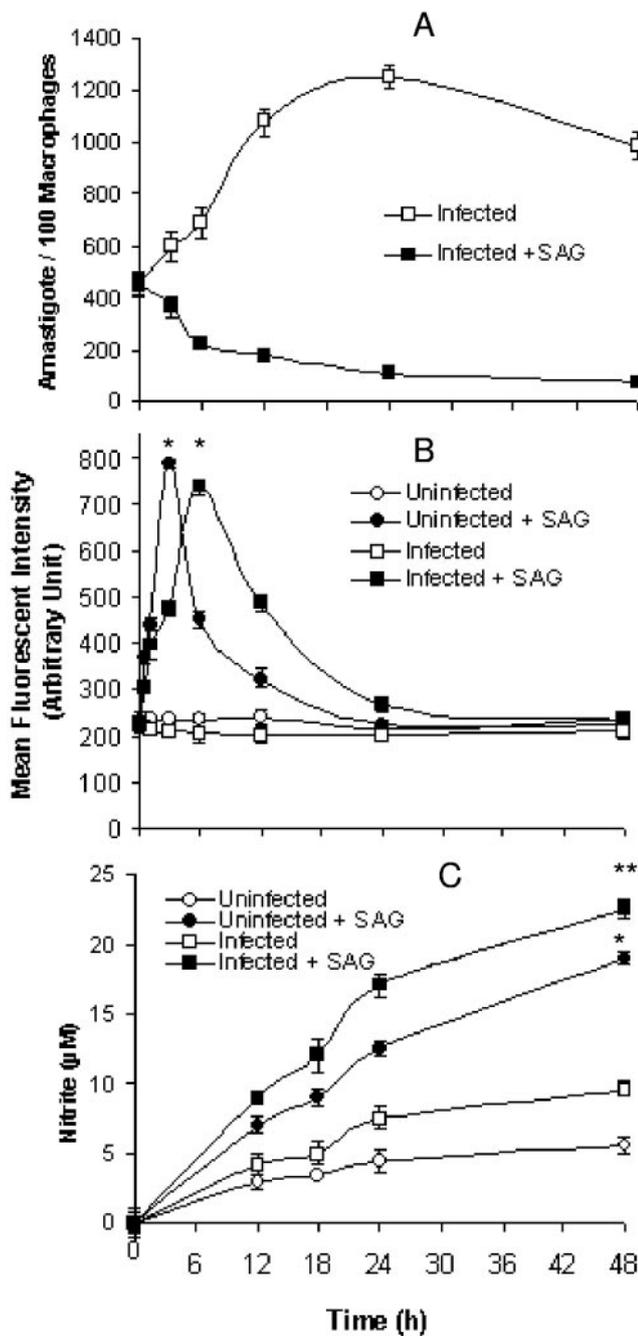
FIG. 1. SAG-induced generation of ROS and NO in Mφs and killing of intracellular parasites. Uninfected Mφs and Mφs infected with *L. donovani* (I-Mφs) were either kept untreated or treated with SAG for different durations. (A) Intracellular parasite numbers were measured for I-Mφs in the absence or presence of SAG. (B) ROS generation was measured with DCFDA; uninfected Mφs and I-Mφs showed significant increases in ROS generation at 3 h and 6 h post-SAG treatment, respectively, compared with levels for corresponding untreated controls (*, $P < 0.001$). (C) Nitrite was measured using Griess reagent in cell-free culture supernatants of SAG-treated uninfected Mφs; I-Mφs showed significant increase in nitrite generation compared to untreated counterparts (*, $P < 0.001$; **, $P < 0.005$). All results are presented as means ± SEM of five independent experiments.

scavenger of ROS, 1 h prior to SAG treatment; this inhibited the SAG-mediated killing of intracellular *L. donovani* at 6 h (i.e., when SAG-mediated ROS generation was highest and NO generation was negligible in I-Mφs) by more than 60% (Fig. 2A). Similar data were also obtained with tocopherol at this time point (unpublished data). For our subsequent experiments concerning ROS generation, we have taken the 6-h posttreatment time point because ROS generation peaked at this point in I-Mφs in response to SAG treatment (Fig. 1B). Since a significant level of NO was produced at 24 h and 48 h (Fig. 1C) in SAG-treated I-Mφs, we assessed the intracellular parasite numbers in the presence or absence of L-NMMA at these time points. Significant ($P < 0.001$) inhibition of SAG-mediated parasite killing occurred in the presence of L-NMMA at 24 h post-SAG treatment, the action being more pronounced at the 48-h time point (Fig. 2A). The role of iNOS2 was demonstrated by the lack of an antileishmanial effect of SAG in iNOS-deficient Mφs at a later phase of infection in vitro (Fig. 2B). It has been shown earlier that CD40-induced expression of iNOS2 is mediated by p38 MAPK activation (31). Therefore, it is quite possible that the SAG-induced NO generation is also dependent on signaling intermediates.

Inhibitors of PI3K, PKC, Ras, and ERKs strongly inhibited SAG-induced ROS generation, while inhibitors of PI3K and p38 MAPK strongly inhibited SAG-induced NO generation. Since ROS generation is reported to involve Ras (54), PI3K (14), PKC (55), and ERKs (14, 54), we tested whether different inhibitors of these intermediates alter the SAG-induced ROS production in Mφs. We observed that treatment of I-Mφs with inhibitors of PI3K (i.e., wortmannin), PKC (i.e., calphostin C), Ras (i.e., mevastatin), or MEK (i.e., U0126) prior to SAG treatment strongly inhibited the SAG-induced ROS generation (Fig. 3, top). Taking the SAG-induced increase in ROS generation over the untreated control value as 100%, the extents of inhibition of ROS generation were ~58.5% with wortmannin, ~74.16% with calphostin C, ~55% with mevastatin, and ~71% with U0126. On the other hand, the inhibitor of p38 MAPK (i.e., SB203580) only marginally (~16.6%) inhibited the SAG-induced ROS generation. This study was carried out at 6 h because maximum ROS generation was observed for I-Mφs at this time point.

The p38 MAPK has widely been reported to be involved in NO generation (3, 25, 31), and activation of p38 MAPK is reported to require the involvement of PI3K (25, 30, 52). Therefore, we tested with inhibitors of PI3K and p38 MAPK to determine whether SAG involves this pathway to induce NO production in Mφs. It was observed that treatment of I-Mφs with wortmannin or SB203580 prior to SAG treatment almost completely inhibited the SAG-induced NO generation at 24 h and also inhibited intracellular parasite killing by ~94% or ~99%, respectively (Fig. 3, bottom). On the contrary, pretreatment with inhibitors of PKC, Ras, and ERKs had only minor inhibitory effects (~5%, ~14.8%, and ~18.9%, respectively) on SAG-induced NO production. This study was also conducted at the 48-h time point, and the results obtained were essentially similar to those obtained at the 24-h time point. However, the result for the 24-h time point has been presented because the difference in numbers of intracellular *L. donovani* parasites between untreated and SAG-treated Mφs was maximal at this time point. Altogether, these data suggest that
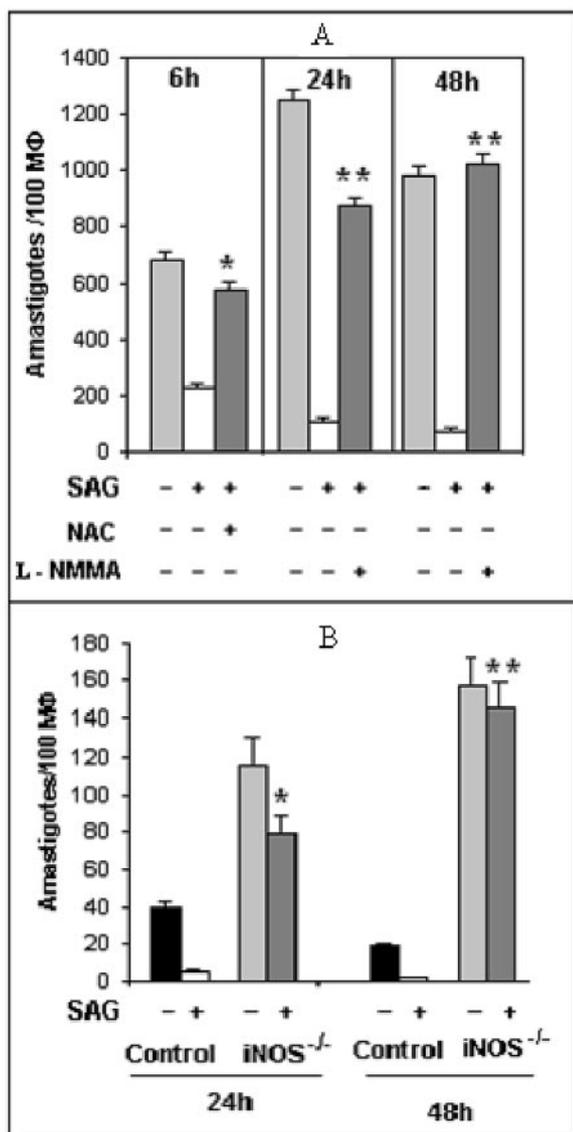
FIG. 2. Effect of NAC (scavenger of ROS) and L-NMMA (competitive inhibitor of iNOS) on SAG-mediated intracellular parasite killing. (A) I-Mϕs cultured on cover glasses were either kept untreated or treated with NAC or L-NMMA prior to SAG treatment. After indicated time points, cover glasses were stained with Giemsa stain and assessed for intracellular parasite number. Pretreatment with NAC and L-NMMA significantly inhibited SAG-mediated parasite killing (*, $P < 0.005$ for NAC; **, $P < 0.001$ for L-NMMA) compared to levels for corresponding SAG-treated controls. Results are presented as means ± SEM of four independent experiments. (B) Peritoneal Mϕs isolated from iNOS$^{-/-}$ and wild-type C57BL/6 mice were cultured on cover glasses, infected with *L. donovani*, and either kept untreated or treated with SAG for 24 h and 48 h, following which their intracellular parasite numbers were assessed. SAG-mediated intracellular *L. donovani* killing was significantly inhibited in infected Mϕs of iNOS$^{-/-}$ mice (*, $P < 0.005$; **, $P < 0.001$). Results are presented as means ± SEM of three independent experiments.
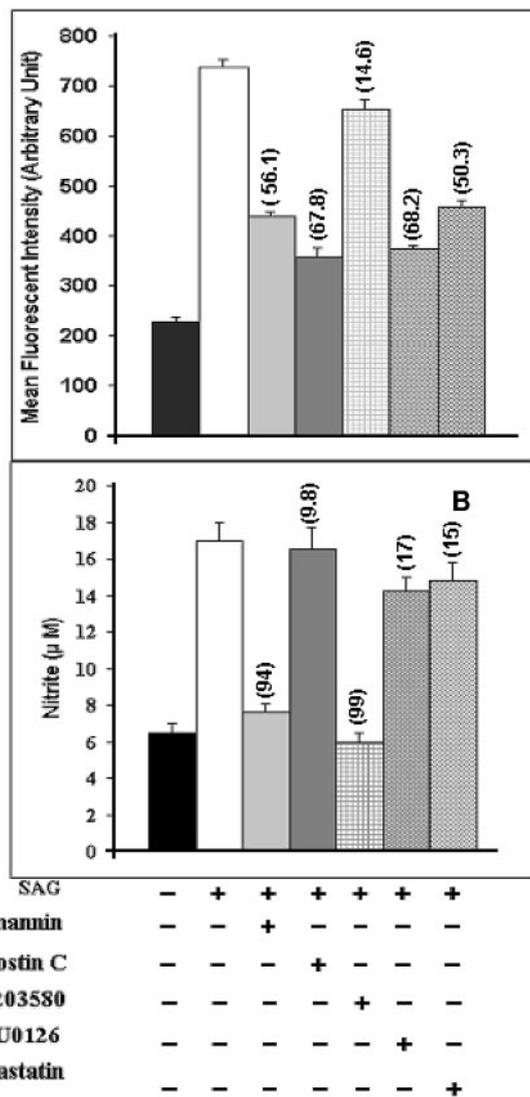
FIG. 3. Effect of inhibitors of PI3K (wortmannin), PKC (calphostin C), Ras (mevastatin), and ERK (U0126) on SAG-induced generation of ROS and that of inhibitor of p38 MAPK (SB203580) on SAG-induced generation of NO. I-Mϕs were treated (+) with wortmannin, calphostin C, mevastatin, U0126, or SB203580 prior to SAG treatment. (Top) ROS levels were measured after 6 h of SAG treatment, and corresponding intracellular parasite numbers were also assessed. Pretreatment with wortmannin, calphostin C, mevastatin, or U0126 significantly inhibited SAG-mediated ROS generation as well as parasite killing ($P < 0.005$). (Bottom) Nitrite levels in cell-free culture supernatant were estimated after 24 h of SAG treatment, and corresponding intracellular parasite numbers were also assessed. Pretreatment with wortmannin or SB203580 significantly inhibited SAG-mediated NO generation as well as parasite killing ($P < 0.001$). For both panels, numbers in parentheses show percentages of inhibition of SAG-mediated intracellular parasite killing compared to levels for respective SAG-treated controls. Results are presented as means ± SEM of five independent experiments. As mentioned in Materials and Methods, the inhibitors did not exhibit any cytotoxicity at the doses used in this and subsequent experiments.

SAG results in activation of PI3K, PKC, Ras, and MEK-1/MEK-2 for ROS generation and that it activates p38 MAPK for NO generation.

SAG treatment induced phosphorylation of PI3K, PDK1, Akt, PKC α/β$_{II}$, Raf, ERKs, and p38 MAPK. After identi-fying the signaling intermediates required for SAG-induced ROS and NO generation, we examined the phosphorylation status of PI3K, PKC, Raf, ERKs, p38 MAPK, and other associated molecules, like phosphoinositide-dependent kinase 1 (PDK1) and Akt, that are intermediates in the p42/44
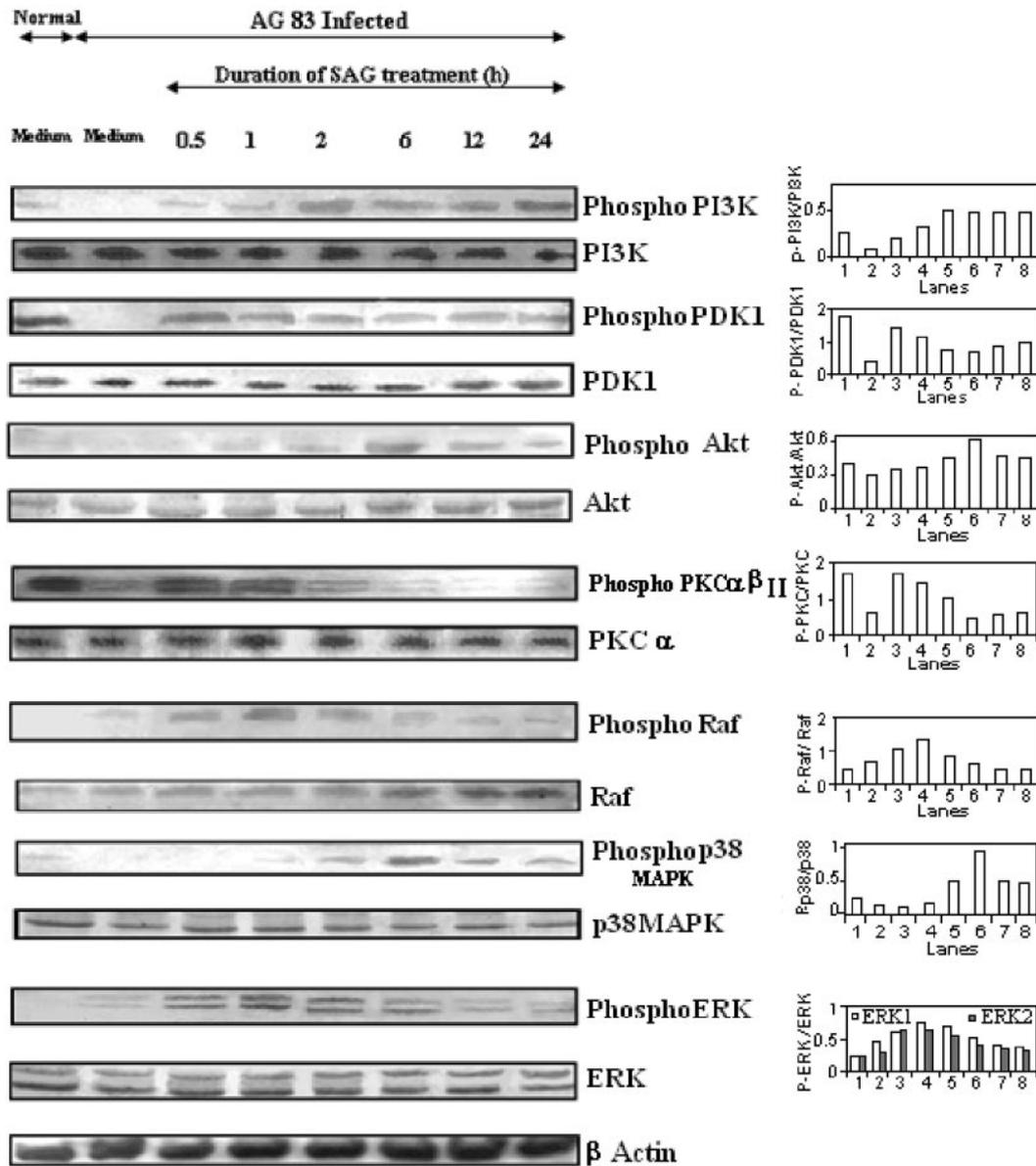
FIG. 4. SAG treatment induces phosphorylation of PI3K, PDK1, Akt, PKC α/β_{II}, Raf, ERK, and p38 MAPK. I-Mϕs were either kept untreated or treated with SAG for different durations; cell lysates were prepared, run in 10% polyacrylamide gels, and immunoblotted with MAbs against whole and phosphorylated forms (labeled Phospho or P) of PI3K, PKC α/β_{II} (phosphorylated form of α/β_{II} and whole α only), PDK1, Raf, ERK-1/ERK-2, p38 MAPK, and Akt, with β-actin as an internal control. The phosphorylation status of each of the above molecules was expressed as the densitometric ratio of the phosphorylated form versus the expression control. Representative data of three similar experiments are presented. AG83, MHOM/IN/1983/AG83.

MAPK and p38 MAPK activation pathways (26, 30, 52). Since PKC α and β are known to be involved in the ERK activation pathway (7, 8), we tested the phosphorylation of PKC α/β_{II} in this study.

It was observed that SAG treatment of I-Mϕs for only 30 min induced the phosphorylation of PI3K, PDK1, PKC α/β_{II}, Raf, and ERKs (Fig. 4). PI3K phosphorylation increased gradually with an increase in duration of SAG treatment up to 2 h and remained high even up to 24 h. The extent of phosphorylation of PI3K following 2 h of SAG treatment was ~4-fold compared to that for the infected control. Phosphorylations of PDK1 and PKC α/β_{II} were

maximal at 30 min post-SAG treatment. The extents of phosphorylation of PDK1 and PKC α/β_{II} following 0.5 h of SAG treatment were ~3-fold and ~2.5-fold, respectively, compared to that for the infected control. Thereafter, the phosphorylation level of PKC α/β_{II} decreased gradually, but the PDK1 phosphorylation was sustained (at an ~2-fold-higher level than that for the infected control, even up to 24 h). Interestingly, Raf phosphorylation, which increased gradually from 30 min with an increase in duration of SAG treatment, remained high even up to 2 h of treatment and then decreased gradually. Strong phosphorylation of ERKs was observed up to 2 h of SAG treatment; it decreased
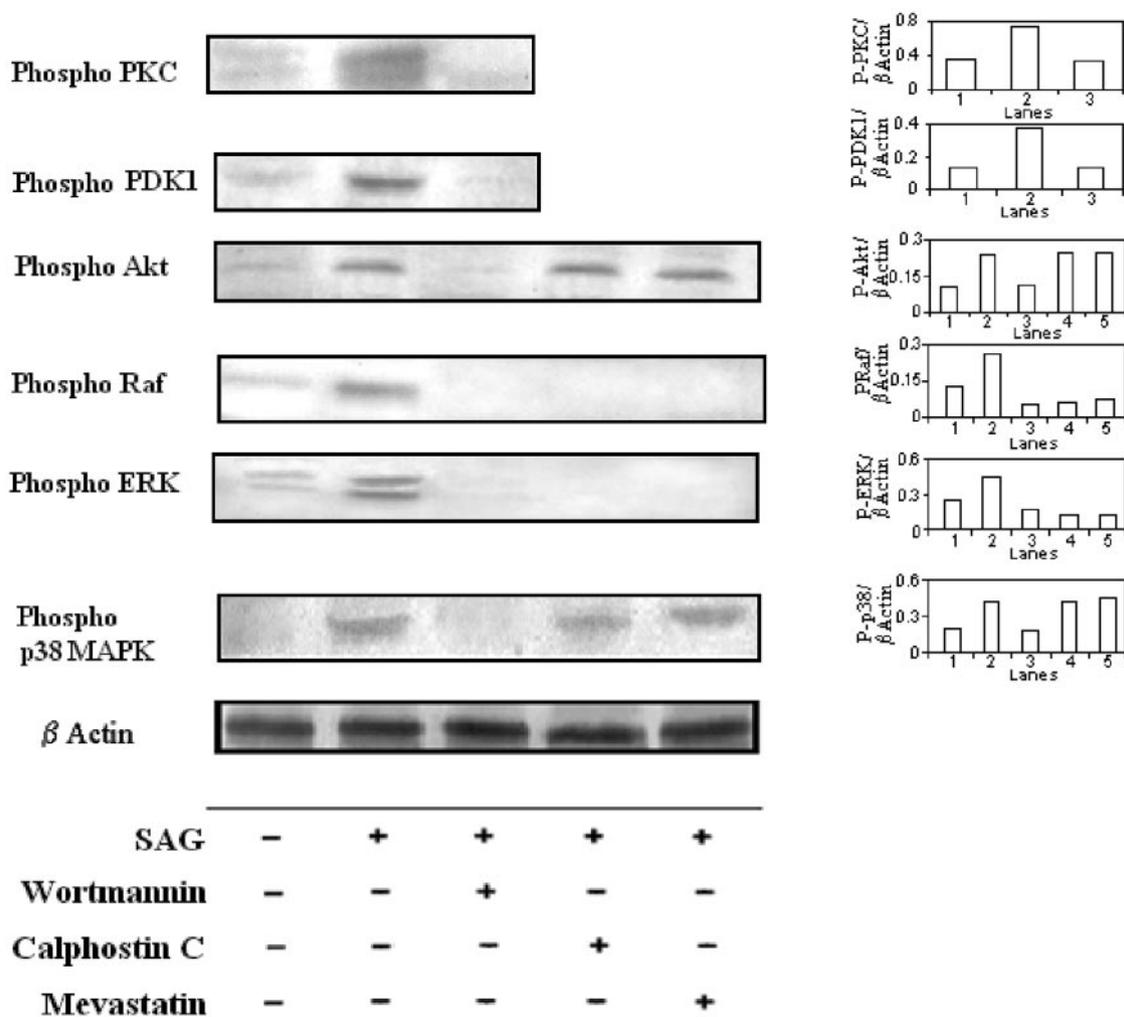
FIG. 5. PI3K phosphorylation due to SAG treatment induces phosphorylation of PDK1, PKC α/β$_{II}$, Raf, and ERK-1/ERK-2 as well as that of Akt and p38 MAPK. I-Mφs were treated with an inhibitor of PI3K (wortmannin), PKC (calphostin C), or Ras (mevastatin) for 1 h prior to SAG treatment, and the phosphorylation status of PDK1 and PKC α/β$_{II}$ at 30 min of SAG treatment, Raf and ERK at 1 h of SAG treatment, and Akt and p38 MAPK at 6 h of SAG treatment (SAG-induced phosphorylation status of each of the above-mentioned signaling molecules was maximal at these time points) was determined by immunoblotting. Phosphorylation status of each of the above-mentioned molecules was expressed as the densitometric ratio of the phosphorylated form (labeled Phospho or P) versus the internal control (β-actin). Representative data of three similar experiments are presented here.

gradually thereafter. The extents of phosphorylation of ERK-1 and ERK-2 following 1 h and 2 h of SAG treatment were 1.5-fold and ~2-fold, respectively, compared to that for the infected control. Phosphorylation of Akt was very weak at 30 min following SAG treatment but increased gradually and reached the peak at about 6 h posttreatment, i.e., when the SAG-induced phosphorylation of PKC α/β$_{II}$ became very weak. The extent of phosphorylation of Akt following 6 h of SAG treatment was ~2-fold compared to that for the infected control. Phosphorylation of p38 MAPK was evident only following 1 h of SAG treatment; it gradually increased up to 6 h and then decreased slightly but persisted even up to 24 h post-SAG treatment (Fig. 4). The peak of phosphorylation of p38 MAPK was observed to occur following 6 h of SAG treatment, and the extent was ~4.5-fold compared to that for the infected control.

To test the probable pathway for SAG-induced phosphory-

lation of ERKs and p38 MAPK in I-Mφs, Western blot experiments were performed with inhibitors of PI3K, PKC, and Ras. We observed that pretreatment with wortmannin completely abrogated SAG-induced PDK1 and PKC α/β$_{II}$ phosphorylation at 30 min and almost completely inhibited the SAG-induced phosphorylations of Raf and ERKs at 1 h (Fig. 5). On the other hand, wortmannin pretreatment also completely abrogated SAG-induced phosphorylation of Akt and almost completely inhibited that of p38 MAPK at 6 h (Fig. 5). Further, pretreatment with calphostin C or mevastatin strongly inhibited SAG-induced phosphorylations of Raf and ERKs at 1 h but not that of Akt or p38 MAPK at 6 h.

SAG treatment triggered TNF-α production through participation of p38 MAPK. Activation of p38 MAPK is well reported to trigger production of TNF-α (29), which is known to induce iNOS2 expression and NO generation (29). These studies prompted us to investigate the involvement of TNF-α in
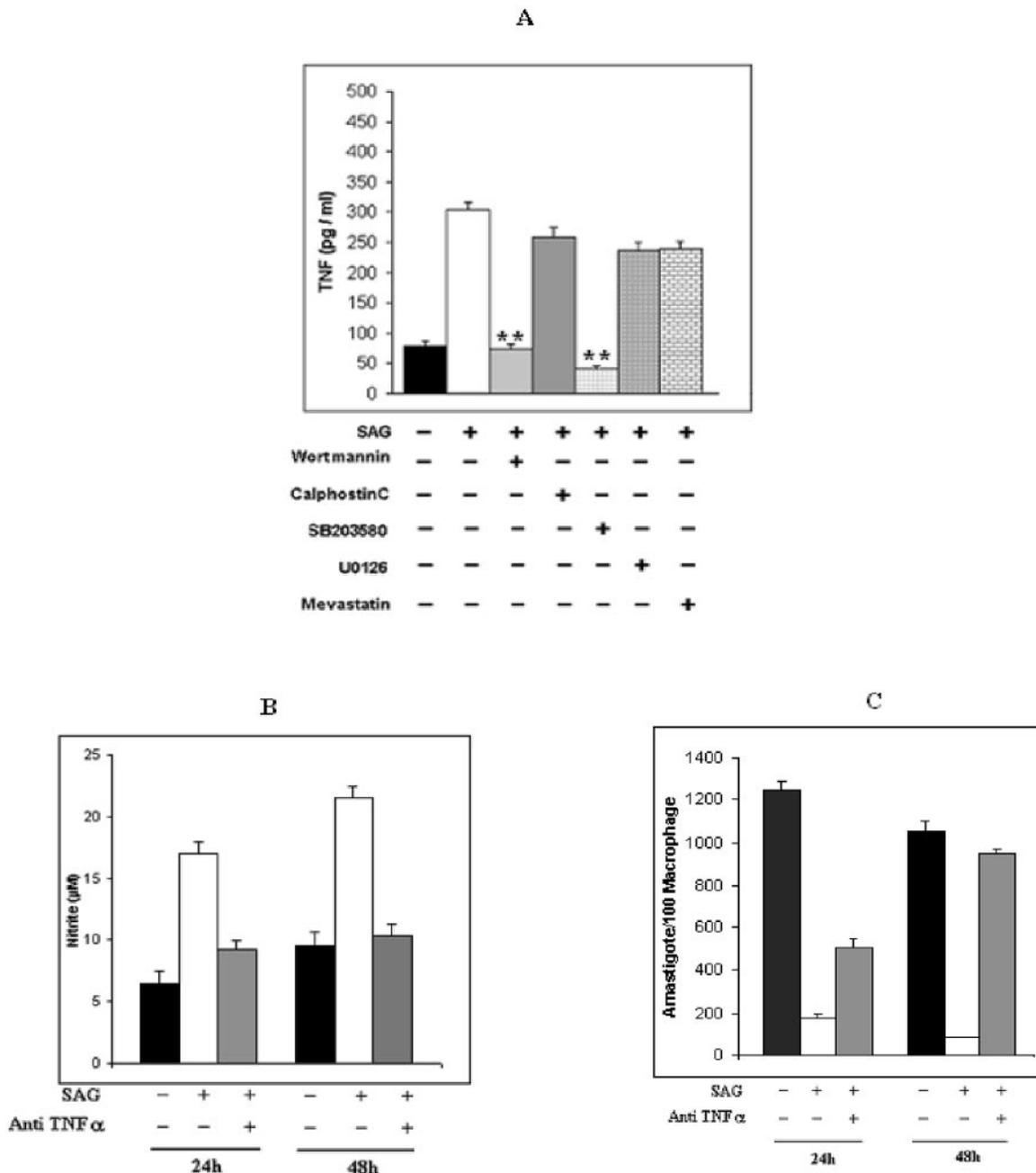
FIG. 6. SAG induces TNF-α production from *L. donovani*-infected Mφs through participation of PI3K and p38 MAPK. (A) I-Mφs were either kept untreated (−) or treated (+) with wortmannin, calphostin C, mevastatin, U0126, or SB203580 prior to SAG treatment; cell-free culture supernatants were collected after 18 h and assayed for TNF-α by sandwich enzyme-linked immunosorbent assay. Pretreatment with wortmannin or SB203580 significantly inhibited SAG-mediated TNF-α generation (**, $P < 0.001$). (B) In some experiments, I-Mφ was either kept untreated or treated with SAG in the presence or absence of neutralizing anti-TNF-α MAb, and resulting levels of nitrite accumulated in cell-free culture supernatants after 24 h of SAG treatment were measured. (C) Corresponding intracellular parasite numbers were also assessed. Neutralization of TNF-α significantly inhibited SAG-mediated NO generation ($P < 0.005$) as well as intracellular *L. donovani* killing ($P < 0.005$ at 24 h). Results presented are means ± SEM of four independent experiments.

the SAG-mediated NO generation due to activation of p38 MAPK.

SAG treatment of I-Mφs induced TNF-α production (Fig. 6A), and this could be inhibited almost completely by pretreatment with wortmannin or SB203580. On the contrary, pretreatment with an inhibitor of PKC, Ras, or ERKs failed to show any

significant inhibition (extent of inhibition was ~7.1%, ~14.6%, or ~12%, respectively) (Fig. 6A). We then investigated whether the SAG-induced NO production in I-Mφs was mediated by TNF-α. It was observed that incubation of I-Mφs with anti-TNF-α neutralizing Ab strongly suppressed SAG-induced NO production after 24 h and completely abrogated it

after 48 h (Fig. 6B). Furthermore, incubation of I-Mϕs with anti-TNF-α neutralizing Ab also inhibited SAG-induced killing of intracellular *L. donovani* parasites partially (~60.8%), but significantly ($P < 0.01$), at 24 h and completely after 48 h ($P < 0.005$) (Fig. 6C).

DISCUSSION

The present study has provided the first insight into the involvement of signaling intermediates, namely, PI3K, PKC, and MAPKs, in SAG-mediated generation of the leishmanicidal molecules (ROS and NO). Our results show that SAG treatment alone induced both ROS and NO in murine Mϕs and induced two waves of killing of *L. donovani* amastigotes. The first phase of killing (i.e., at an early time point, around 6 h posttreatment) was due to induction of ROS, as evident from the sensitivity to tocopherol (data not shown) or NAC, while the second wave of killing (i.e., at later time points, 24 h and 48 h) was mediated by NO generation, as evident from the sensitivity to L-NMMA and failure of SAG to inhibit killing of intracellular *L. donovani* parasite replication in peritoneal Mϕs from iNOS$^{-/-}$ C57BL/6 mice at 24 h posttreatment. Both ROS and NO are known to be involved in parasite killing in the early stage of leishmanial infection in mice, whereas NO alone is involved in the late phase (39).

Since the SAG-induced phosphorylation of PKC α/β_{II}, which occurred by 30 min posttreatment, was observed to be inhibited by wortmannin pretreatment, it is possible that SAG treatment resulted in rapid phosphorylation of PI3K, which is a well-known activator of PDK1 (9, 27) that in turn activates several PKC isotypes (9, 27). Inasmuch as wortmannin, calphostin C, and mevastatin inhibited the SAG-induced Raf phosphorylation as late as 1 h, our observations present a new mode of Raf activation which is very different from receptor activation-mediated Raf activation and recruitment to the membrane. Our results also suggest that SAG-induced activation of the PI3K-PKC-Ras/Raf pathway triggered ERK phosphorylation. Pretreatment of I-Mϕ with any of these inhibitors or U0126 resulted in significant inhibition ($P < 0.01$ for wortmannin and mevastatin and $P < 0.005$ for calphostin C and U0126) of SAG-mediated ROS generation, suggesting that SAG activates the PI3K-PKC-Ras-ERK pathway and thereby triggers ROS generation.

On the other hand, inhibition of PI3K or p38 MAPK strongly abrogated SAG-mediated NO production in I-Mϕs as well as parasite killing at ~24 h following SAG treatment. This suggested that NO production and subsequent parasite killing in response to SAG treatment involved mainly PI3K and p38 MAPK. The PI3K-Akt-p38 MAPK pathway (25) was shown to be involved in NO generation (25, 26). Activation of PKC inhibits PI3K-mediated activation of Akt (33). In our study it has also been observed that although Akt was phosphorylated 1 h following SAG treatment, the level reached a peak at 6 h posttreatment, when phosphorylation of PKC α/β_{II} was very low. This phosphorylation could be inhibited by wortmannin pretreatment, confirming that SAG-induced prolonged activation of PI3K resulted in Akt phosphorylation. The activation of the PI3K-Akt pathway by SAG seemed to trigger phosphorylation of p38 MAPK that was almost completely abrogated by wortmannin pretreatment. The PKC-Ras pathway played a

minimal role in SAG-induced p38 MAPK phosphorylation, as it was insensitive to pretreatment with calphostin C or mevastatin.

L. donovani infection has been reported to increase protein tyrosine phosphatase activity, mainly that of type SHP1 (5, 44–46), which might contribute to dysregulation of protein tyrosine kinase-dependent signaling events and Mϕ deactivation (44). SHP1 might directly dephosphorylate ERKs (45) and regulate activation of other important signaling molecules, like PI3K (12). Thus, inhibition of SHP1 by SAG might indirectly favor the tyrosine phosphorylation of PI3K and might thereby help in activating both the PI3K–PKC–Ras/Raf–ERK-1/ERK-2 pathway for ROS generation and the PI3K-Akt-p38 MAPK pathway leading to NO generation.

The p38 MAPK has been shown to induce TNF-α production (29), which in turn induces iNOS2 expression and subsequent NO generation (29), as suggested by the inhibition of NO generation and parasite killing by treatment with anti-TNF-α neutralizing Ab. The SAG-mediated TNF-α generation could be inhibited by wortmannin or SB203580 pretreatment, indicating that SAG-induced activation of the PI3K-p38 MAPK pathway not only activates NO-mediated parasite control but also reinforces the mechanism by triggering endogenous TNF-α that controls the parasite in an autocrine manner. Indeed, the SAG-induced antileishmanial activity is reduced in TNF-α knockout mice (35). In addition, since SAG up-regulates IFN-γ receptors in both uninfected and *L. donovani*-infected THP-1 cells, as well as in monocytes derived from kala-azar patients treated with SAG (13), it is quite possible that SAG influences the host's antileishmanial defense by altering IFN-γ responsiveness. Indeed, SAG fails to act in IFN-γ knockout mice (40), and in the case of chronic, nonhealing murine cutaneous leishmaniasis, treatment with SAG plus IFN-γ induces much higher levels of iNOS2 transcripts in footpad tissues than SAG or IFN-γ alone (28). We have also observed that SAG and IFN-γ synergize to produce high levels of NO in Mϕs (unpublished data). A combination of SAG and IFN-γ is also known to be therapeutically much more effective than SAG alone in the treatment of visceral leishmaniasis (37). We have further observed that SAG triggers production of IL-12 in both uninfected Mϕs and I-Mϕs (unpublished data). IL-12 is known to induce Th cells to produce IFN-γ, which in turn activates Mϕs to produce TNF-α and, subsequently, NO. This might explain the failure of SAG to act in IL-12 knockout mice, as reported in earlier studies (41). Furthermore, an earlier study showed that SAG treatment of infected mice imparted resistance to reinfection whereas SAG treatment prior to infection imparted partial resistance to *L. donovani* infection (10). All of these results may explain the requirement of T cells for the activity of SAG in vivo (36). Interestingly, neither sodium gluconate (i.e., the organic backbone of SAG) nor inorganic Sb^V (SbCl$_5$) could induce significant levels of ROS or NO generation and parasite killing in I-Mϕs, while SbCl$_5$ (at 10 μg Sb^V equivalent) proved to be highly cytotoxic (unpublished data), suggesting that neither the backbone nor the metalloid alone has the immunomodulatory effect shown by SAG (an organic chelate of Sb^V). Therefore, the use of SAG in combination therapy (either with other drugs or possibly with vaccines) may prove beneficial. Moreover, our preliminary observations indicate that resistance to antimonials occurred mainly due to overexpression

of MRP1 on the host cell surface and consequent nonretention of antimony by host cells harboring antimony-resistant strains of *L. donovani* (unpublished observation), suggesting that the use of suitable resistance-modifying agents might sensitize Sb-resistant cases to SAG treatment. Further studies in this direction are being pursued.

REFERENCES

1. **Alexander, J., K. C. Carter, N. Al-Fasi, A. Satoskar, and F. Brombacher.** 2000. Endogenous IL-4 is necessary for effective drug therapy against visceral leishmaniasis. Eur. J. Immunol. **30:**2935–2943.
2. **Amer, A. O., and M. S. Swanson.** 2002. Phagosome of one's own: a microbial guide to life in the macrophage. Curr. Opin. Microbiol. **5:**56–61.
3. **Awasthi, A., R. Mathur, A. Khan, B. N. Joshi, N. Jain, S. Sawant, R. Boppana, D. Mitra, and B. Saha.** 2003. CD40 signaling is impaired in L. major-infected macrophages and is rescued by a p38MAPK activator establishing a host-protective memory T cell response. J. Exp. Med. **197:**1037–1043.
4. **Berman, J. D., and D. J. Wyler.** 1980. An in vitro model for investigation of chemotherapeutic agents in leishmaniasis. J. Infect. Dis. **142:**83–86.
5. **Blanchette, J., N. Racette, R. Faure, K. A. Siminovitch, and M. Olivier.** 1999. *Leishmania*-induced increases in activation of macrophage SHP-1 tyrosine phosphatase are associated with impaired IFN-gamma-triggered JAK2 activation. Eur. J. Immunol. **29:**3737–3744.
6. **Brahmachari, U. N.** 1922. Chemotherapy of antimonial compounds in kala-azar infection. Part I. Indian J. Med. Res. **10:**492–498.
7. **Breton, A., A. Descoteaux, S. W. Lee, H. B. Kwak, W. J. Chung, H. Cheong, H. H. Kim, and Z. H. Lee.** 2003. Participation of protein kinase C beta in osteoclast differentiation and function. Bone **32:**217–227.
8. **Breton, A., and A. Descoteaux.** 2000. Protein kinase C-alpha participates in FcgammaR-mediated phagocytosis in macrophages. Biochem. Biophys. Res. Commun. **276:**472–476.
9. **Cantrell, D. A.** 2001. Phosphoinositide 3-kinase signalling pathways. J. Cell Sci. **114:**1439–1445.
10. **Carter, K. C., J. Alexander, A. J. Baillie, and T. F. Dolan.** 1989. Visceral leishmaniasis: resistance to reinfection in the liver following chemotherapy in the BALB/c mouse. Exp. Parasitol. **68:**375–381.
11. **Chakraborty, D., S. Banerjee, A. Sen, K. K. Banerjee, P. Das, and S. Roy.** 2005. *Leishmania donovani* affects antigen presentation of macrophage by disrupting lipid rafts. J. Immunol. **175:**3214–3224.
12. **Cuevas, P., Y. Lu, S. Watt, R. Kumar, J. Zhang, K. A. Siminovitch, and G. B. Mills.** 1999. SHP-1 regulates Lck-induced phosphatidylinositol 3-kinase phosphorylation and activity. J. Biol. Chem. **274:**27583–27589.
13. **Dasgupta, B., K. Roychoudhury, S. Ganguly, P. Kumar Sinha, P. Das, and S. Roy.** 2003. Antileishmanial drugs cause up-regulation of interferon-gamma receptor 1, not only in the monocytes of visceral leishmaniasis cases but also in cultured THP1 cells. Ann. Trop. Med. Parasitol. **97:**245–257.
14. **Dreiem, A., O. Myhre, and F. Fonnum.** 2003. Involvement of the extracellular signal regulated kinase pathway in hydrocarbon-induced reactive oxygen species formation in human neutrophil granulocytes. Toxicol. Appl. Pharmacol. **190:**102–110.
15. **Escobar, P., V. Yardley, and S. L. Croft.** 2001. Activities of hexadecylphosphocholine (miltefosine), AmBisome, and sodium stibogluconate (Pentostam) against *Leishmania donovani* in immunodeficient *scid* mice. Antimicrob. Agents Chemother. **45:**1872–1875.
16. **Favata, M. F., K. Y. Horiuchi, E. J. Manos, A. J. Daulerio, D. A. Stradley, W. S. Feeser, D. E. Van Dyk, W. J. Pitts, R. A. Earl, F. Hobbs, R. A. Copeland, R. L. Magolda, P. A. Scherle, and J. M. Trzaskos.** 1998. Identification of a novel inhibitor of mitogen-activated protein kinase kinase. J. Biol. Chem. **273:**18623–18632.
17. **Fernandez-Guerrero, M. L., J. M. Aguado, L. Buzon, C. Barros, C. Montalban, T. Martin, and E. Bouza.** 1987. Visceral leishmaniasis in immunocompromised hosts. Am. J. Med. **83:**1098–1102.
18. **Ghose, A. C., A. Mookerjee, K. Sengupta, and A. K. Ghosh.** 1999. Therapeutic and prophylactic uses of protein A in the control of *Leishmania donovani* infection in experimental animals. Immunol. Lett. **65:**175–181.
19. **Green, L. C., D. A. Wagner, J. Glogowski, P. L. Skipper, J. S. Wishnok, and**

20. **S. R. Tannenbaum.** 1982. Analysis of nitrate, nitrite, and [15N]nitrate in biological fluids. Anal. Biochem. **126:**131–138.
21. **Herwaldt, B. L.** 1999. Leishmaniasis. Lancet **354:**1191–1199.
22. **Hirji, N., T. J. Lin, E. Bissonnette, M. Belosevic, and A. D. Befus.** 1998. Mechanisms of macrophage stimulation through CD8: macrophage CD8 and CD8β induce nitric oxide production and associated killing of the parasite *Leishmania major*. J. Immunol. **160:**6004–6011.
23. **Ibrahim, M. E., M. Hag-Ali, A. M. el-Hassan, T. G. Theander, and A. Kharazmi.** 1994. *Leishmania* resistant to sodium stibogluconate: drug-associated macrophage-dependent killing. Parasitol. Res. **80:**569–574.
24. **Jarvis, W. D., A. J. Turner, L. F. Povirk, R. S. Traylor, and S. Grant.** 1994. Induction of apoptotic DNA fragmentation and cell death in HL-60 human promyelocytic leukemia cells by pharmacological inhibitors of protein kinase C. Cancer Res. **54:**1707–1714.
25. **Kao, S. J., H. C. Lei, C. T. Kuo, M. S. Chang, B. C. Chen, Y. C. Chang, W. T. Chiu, and C. H. Lin.** 2005. Lipoteichoic acid induces nuclear factor-kappaB activation and nitric oxide synthase expression via phosphatidylinositol 3-kinase, Akt, and p38 MAPK in RAW 264.7 macrophages. Immunology **115:**366–374.
26. **Lee, H. M., H. S. Jin, J. W. Park, S. M. Park, H. K. Jeon, and T. H. Lee.** 2003. IL-4 augments anisomycin-induced p38 activation via Akt pathway in a follicular dendritic cell (FDC)-like line. FEBS Lett. **549:**110–114.
27. **Le Good, J. A., W. H. Ziegler, D. B. Parekh, D. R. Alessi, P. Cohen, and P. J. Parker.** 1998. Protein kinase C isotypes controlled by phosphoinositide 3-kinase through the protein kinase PDK1. Science **281:**2042–2045.
28. **Li, J., S. Sutterwala, and J. P. Farrell.** 1997. Successful chemotherapy of chronic, nonhealing murine leishmaniasis with sodium stibogluconate and gamma interferon depends on continued interleukin-12 production. Infect. Immun. **65:**3225–3230.
29. **Li, Y., R. F. Schwabe, T. DeVries-Seimon, P. M. Yao, M. C. Gerbod-Giannone, A. R. Tall, R. J. Davis, R. Flavell, D. A. Brenner, and I. Tabas.** 2005. Free cholesterol-loaded macrophages are an abundant source of tumor necrosis factor-alpha and interleukin-6: model of NF-kappaB- and MAP kinase-dependent inflammation in advanced atherosclerosis. J. Biol. Chem. **280:**21763–21772.
30. **Madrid, L. V., M. W. Mayo, J. Y. Reuther, and A. S. Baldwin, Jr.** 2001. Akt stimulates the transactivation potential of the RelA/p65 subunit of NF-kappa B through utilization of the Ikappa B kinase and activation of the mitogen-activated protein kinase p38. J. Biol. Chem. **276:**18934–18940.
31. **Mathur, R. K., A. Awasthi, P. Wadhone, B. Ramanamurthy, and B. Saha.** 2004. Reciprocal CD40 signals through p38MAPK and ERK-1/2 induce counteracting immune responses. Nat. Med. **10:**540–544.
32. **Mookerjee, A., P. C. Sen, and A. C. Ghose.** 2003. Immunosuppression in hamsters with progressive visceral leishmaniasis is associated with an impairment of protein kinase C activity in their lymphocytes that can be partially reversed by okadaic acid or anti-transforming growth factor β antibody. Infect. Immun. **71:**2439–2446.
33. **Motley, E. D., S. M. Kabir, C. D. Gardner, K. Eguchi, G. D. Frank, T. Kuroki, M. Ohba, T. Yamakawa, and S. Eguchi.** 2002. Lysophosphatidylcholine inhibits insulin-induced Akt activation through protein kinase C-alpha in vascular smooth muscle cells. Hypertension **39:**508–512.
34. **Murray, H. W., G. D. Miralles, M. Y. Stoeckle, and D. F. McDermott.** 1993. Role and effect of IL-2 in experimental visceral leishmaniasis. J. Immunol. **151:**929–938.
35. **Murray, H. W., A. Jungbluth, E. Ritter, C. Montelibano, and M. W. Marino.** 2000. Visceral leishmaniasis in mice devoid of tumor necrosis factor and response to treatment. Infect. Immun. **68:**6289–6293.
36. **Murray, H. W., M. J. Oca, A. M. Granger, and R. D. Schreiber.** 1989. Requirement for T cells and effect of lymphokines in successful chemotherapy for an intracellular infection. Experimental visceral leishmaniasis. J. Clin. Invest. **83:**1253–1257.
37. **Murray, H. W., J. D. Berman, and S. D. Wright.** 1988. Immunochemotherapy for intracellular *Leishmania donovani* infection: gamma interferon plus pentavalent antimony. J. Infect. Dis. **157:**973–978.
38. **Murray, H. W.** 1999. Kala-azar as an AIDS-related opportunistic infection. AIDS Patient Care STDs **13:**459–465.
39. **Murray, H. W., and C. F. Nathan.** 1999. Macrophage microbicidal mechanisms in vivo: reactive nitrogen versus oxygen intermediates in the killing of intracellular visceral *Leishmania donovani*. J. Exp. Med. **189:**741–746.
40. **Murray, H. W., and S. Delph-Etienne.** 2000. Roles of endogenous gamma interferon and macrophage microbicidal mechanisms in host response to chemotherapy in experimental visceral leishmaniasis. Infect. Immun. **68:**288–293.
41. **Murray, H. W., C. Montelibano, R. Peterson, and J. P. Sypek.** 2000. Interleukin-12 regulates the response to chemotherapy in experimental visceral leishmaniasis. J. Infect. Dis. **182:**1497–1502.
42. **Murray, H. W., J. D. Berman, C. R. Davies, and N. G. Saravia.** 2005. Advances in leishmaniasis. Lancet **366:**1561–1577.

43. **Nabors, G. S., and J. P. Farrell.** 1994. Depletion of interleukin-4 in BALB/c mice with established *Leishmania major* infections increases the efficacy of antimony therapy and promotes Th1-like responses. Infect. Immun. **62:**5498–5504.

44. **Nandan, D., and N. E. Reiner.** 2005. *Leishmania donovani* engages in regulatory interference by targeting macrophage protein tyrosine phosphatase SHP-1. Clin. Immunol. **114:**266–277.

45. **Olivier, M., D. J. Gregory, and G. Forget.** 2005. Subversion mechanisms by which *Leishmania* parasites can escape the host immune response: a signaling point of view. Clin. Microbiol. Rev. **18:**293–305.

46. **Pathak, M. K., and T. Yi.** 2001. Sodium stibogluconate is a potent inhibitor of protein tyrosine phosphatases and augments cytokine responses in hemopoietic cell lines. J. Immunol. **167:**3391–3397.

47. **Prive, C., and A. Descoteaux.** 2000. *Leishmania donovani* promastigotes evade the activation of mitogen-activated protein kinases p38, c-Jun N-terminal kinase, and extracellular signal-regulated kinase-1/2 during infection of naive macrophages. Eur. J. Immunol. **30:**2235–2244.

48. **Rais, S., A. Perianin, M. Lenoir, A. Sadak, D. Rivollet, M. Paul, and M. Deniau.** 2000. Sodium stibogluconate (Pentostam) potentiates oxidant production in murine visceral leishmaniasis and in human blood. Antimicrob. Agents Chemother. **44:**2406–2410.

49. **Roberts, W. L., J. D. Berman, and P. M. Rainey.** 1995. In vitro antileishmanial properties of tri- and pentavalent antimonial preparations. Antimicrob. Agents Chemother. **39:**1234–1239.

50. **Saha, B., H. Nanda-Roy, A. Pakrashi, R. N. Chakrabarti, and S. Roy.** 1991. Immunobiological studies on experimental visceral leishmaniasis. I. Changes in lymphoid organs and their possible role in pathogenesis. Eur. J. Immunol. **21:**577–581.

51. **Saha, B., D. Bandyopadhyay, and S. Roy.** 1995. Immunobiological studies on experimental visceral leishmaniasis. IV. Kinetics of evolution of disease-promoting versus host-protective cells of monocyte-macrophage lineage and their characterization. Scand. J. Immunol. **42:**540–546.

52. **Sato, S., N. Fujita, and T. Tsuruo.** 2004. Involvement of 3-phosphoinositide-dependent protein kinase-1 in the MEK/MAPK signal transduction pathway. J. Biol. Chem. **279:**33759–33767.

53. **Schreck, R., and P. A. Baeuerle.** 1994. Assessing oxygen radicals as mediators in activation of inducible eukaryotic transcription factor NF-kappa B. Methods Enzymol. **234:**151–163.

54. **Seru, R., P. Mondola, S. Damiano, S. Svegliati, S. Agnese, E. V. Avvedimento, and M. Santillo.** 2004. HaRas activates the NADPH oxidase complex in human neuroblastoma cells via extracellular signal-regulated kinase 1/2 pathway. J. Neurochem. **91:**613–622.

55. **Vladimirova, O., F. M. Lu, L. Shawver, and B. Kalman.** 1999. The activation of protein kinase C induces higher production of reactive oxygen species by mononuclear cells in patients with multiple sclerosis than in controls. Inflamm. Res. **48:**412–416.

56. **Yi, T., M. K. Pathak, D. J. Lindner, M. E. Ketterer, C. Farver, and E. C. Borden.** 2002. Anticancer activity of sodium stibogluconate in synergy with IFNs. J. Immunol. **169:**5978–5985.